Optimization of Coke Oven Gas Desulphurization and Combined Cycle Power Plant Electricity Generation

Authors:

LINGYAN DENG, Thomas A. Adams II

Date Submitted: 2018-09-12

Keywords: carbon tax, net present value, desulphurization, coke oven gas valorization, combined cycle power plant, steel refinery, Optimization

Abstract:

Many steel refineries generate significant quantities of coke oven gas (COG), which is in some cases used only to generate low pressure steam and small amounts of electric power. In order to improve energy efficiency and reduce net greenhouse gas emissions, a combined cycle power plant (CCPP) where COG is used as fuel is proposed. However, desulphurization is necessary before the COG can be used as a fuel input for CCPP. Using a local steel refinery as a case study, a proposed desulphurization process is designed to limit the H2S content in COG to less than 1 ppmv, and simulated using ProMax. In addition, the proposed CCPP plant is simulated in Aspen Plus and is optimized using GAMS to global optimality with net present value as the objective function. Furthermore, carbon tax is considered in this study. The optimized CCPP plant was observed to generate more than twice the electrical efficiency when compared to the status quo for the existing steel refinery. Thus, by generating more electricity within the plant gate, the need to purchase electricity reduces and hence reducing lifecycle CO2 emissions considerably.

Record Type: Preprint

Submitted To: LAPSE (Living Archive for Process Systems Engineering)

Citation (overall record, always the latest version): LAPSE:2018.0443
Citation (this specific file, latest version): LAPSE:2018.0443-1
Citation (this specific file, this version): LAPSE:2018.0443-1v2

DOI of Published Version: https://doi.org/10.1021/acs.iecr.8b00246

Optimization of Coke Oven Gas Desulphurization and Combined Cycle Power Plant Electricity Generation

Lingyan Deng, and Thomas A. Adams II*

Department of Chemical Engineering, McMaster University, 1280 Main St. West, Hamilton, Ontario L8S 4L7, Canada

**Corresponding author. Tel.:+1 905 525 9140 ext.24782 E-Mail address: tadams@mcmaster.ca*

Abstract: Many steel refineries generate significant quantities of coke oven gas (COG), which is in some cases used only to generate low pressure steam and small amounts of electric power. In order to improve energy efficiency and reduce net greenhouse gas emissions, a combined cycle power plant (CCPP) where COG is used as fuel is proposed. However, desulphurization is necessary before the COG can be used as a fuel input for CCPP. Using a local steel refinery as a case study, a proposed desulphurization process is designed to limit the H_2S content in COG to less than 1 ppmv, and simulated using ProMax. In addition, the proposed CCPP plant is simulated in Aspen Plus and is optimized using GAMS to global optimality with net present value as the objective function. Furthermore, carbon tax is considered in this study. The optimized CCPP plant was observed to generate more than twice the electrical efficiency when compared to the status quo for the existing steel refinery. Thus, by generating more electricity within the plant gate, the need to purchase electricity reduces and hence reducing lifecycle CO_2 emissions considerably.

Keywords: desulphurization, coke oven gas valorization, combined cycle power plant, steel refinery, optimization, carbon taxes, net present value.

1. Introduction

The steel industry faces significant challenges with high greenhouse gas (GHG) emissions arising from the use of carbon as a required reagent in the primary iron oxide reduction step of the steelmaking process. For example, the ArcelorMittal Dofasco (AMD) refinery in Hamilton, Ontario, Canada, which produces 4.5 million tonnes of steel per year, also emits about 5.0 million tonnes of CO_2 equivalents (CO_2e) per year [1]. As the largest steel making company in Ontario, it is the largest single emitter of CO_2 in this province, emitting 75.0% more GHGs than the second and third largest emitters (which are also steel refineries) [2]. Moreover, the Canadian government has proposed a minimum carbon tax scheme in which CO_2 emissions would be taxed at $10/tonne in 2018, rising to $50/tonne in 2022 [3]. This translates to an extra $250 million per year in taxes for the refinery, which has serious implications on the profitability of the business and therefore incentivizes steel refineries to reduce their emissions wherever possible.

One of the primary sources of CO_2 emissions from steel refineries is associated with the large amounts of by-product gases, such as coke oven gas (COG), blast furnace gas (BFG), and basic oxygen furnace gas (BOFG). Traditionally, these by-product gases are recycled or reused where possible for heat or for metallurgical purposes, or flared for disposal when reuse is not possible. However, these gases potentially have a much higher value, which is often not exploited in practice. For example, Ghanbari et al. [4, 5] and Bermudez et al. [6] examined several different ways of producing synthesis gas from various by-product gases. When properly cleaned and upgraded, off-gases can be converted into more valuable products using the right kind of catalysts, thus creating a wide variety of chemicals and fuels. This concept is known as off-gas valorization. However, there is not always a business case for this, depending on the jurisdiction and situation of each refinery. An older but still relevant benchmark study of the Iron and Steel Industry in Canada found that the average efficiency improvement potential from off-gas valorization is between 20.0% to 30.0% [7].

China produces about 50.0% of the world's crude steel [8], and as such, China has the most industrial experience in utilizing steelmaking off-gas. Chinese steel manufacturers developed various options of utilizing their off-gases, especially coke oven gas (COG). COG is either used as fuel in combined cycle power plant [9-11], for methanol synthesis [12, 13], for natural gas synthesis [14], or as a source of H_2 through extraction [6, 15]. However, these processes are widely different and are currently in various stages of development. Though the COG used for methanol synthesis has been commercialized

successfully since 2004 in China, there is less of a business case for this in other countries using current technology.

The status quo of the AMD refinery in Hamilton and many of its Chinese counterparts is to use COG combustion to generate low pressure steam to power steam turbines (generating electricity), or for other process needs [11]. However, the efficiency is usually low, at about 15.0% by higher heating value (HHV). Therefore, in order to increase the thermal efficiency, an optimized combined cycle power plant (CCPP) for COG is proposed in this work using the AMD Hamilton refinery as a case study. Although there are steel refineries in Brazil [16] and China [10] which use CCPPs powered by a mixture of BFG and COG, a COG-only CCPP had only been studied from a simulation standpoint [9]. Furthermore, there is no previous study found in the literature where an optimal design of a COG-based CCPP system as a whole was carried out to the best of our knowledge. In addition, this is the first work to quantify both the economic and environmental benefits of avoiding grid electricity use by switching to the COG-based CCPP system in the Canadian context. The geographical context is important because the benefits of the proposed system are strongly dependent on the price of grid electricity, and local carbon emissions taxes or regulations. Because of this, the analysis in this paper considers the various trade-offs of applying the CCPP system at different electricity prices and carbon emission taxes.

2. Methodology

2.1. Available Gas Qualities

Typical conditions of available COG are shown in Table 1 [15, 17]. Note that COG has about half of the high heating value of natural gas (950-1150 Btu/ft^3) [18], which is high enough to use for combustion-based electricity generation. This work uses COG flow rates and qualities provided by AMD Hamilton, but for confidentiality reasons, only ranges and/or normalized data are reported in this paper when referring to existing commercial processes. For a sense of scale, the flow rate of the COG is enough to produce on the order of 20.0-80.0 MW of electric power with the classic steam cycle and is available in approximately continuous amounts.

Table 1. Typical characteristics of available coke oven gas.

Component	COG
Temperature (°C)	35.0
Pressure (bar)	1.44

HHV (Btu/ft^3)	400-570
HHV (MJ/kg)	22.6-32.4
Chemical Composition (volume fraction)	
%C_2H_2	1.50-3.00
%CH_4	22.0-28.0
%CO	5.00-9.00
%CO_2	1.00-3.50
%H_2	45.0-60.0
%N_2	3.00-6.00
%O_2	0.100-1.00
H_2S (ppmv)	3420-4140
CS_2 (ppmv)	82.0-92.0
Thiophene (C_4H_4S) (ppmv)	26.0-34.0

2.2. COG Desulphurization

The COG at AMD Hamilton contains H_2S, CS_2, and thiophene (C_4H_4S) with approximate ranges shown in Table 1. Typically, these sulfur compounds need to be removed before COG can be used for combustion or other purposes. Currently, the status quo at AMD Hamilton is to use a sulfur removal process that removes some, but not all, of the sulfur compounds. However, in the proposed CCPP design, the COG is combusted at high-pressure, which requires the COG to be much sweeter. The maximum H_2S concentration that can be tolerated is 4 ppmv as a design requirement [19] which is a three-order-of-magnitude reduction in sulfur content. Therefore, we have designed and simulated a sulfur removal system that is different from the process used at AMD Hamilton to sweeten the COG to the acceptable levels.

Our proposed COG-sweetening system is designed for H_2S removal only. Thiophene is a heterocyclic compound and has very stable chemical bonds, and is commonly removed from oil and coal by hydro-desulfurization processes at high pressure [20]. A much more expensive two-stage hydro-desulfurization step is required [21] to remove thiophene from COG. For the case study of AMD Hamilton, removing mainly the H_2S and some CS_2 at the same time is sufficient to meet environmental emission standards of the post-combustion flue gas and avoid damage to the equipment [22]. Therefore, thiophene removal is not studied in this work.

Four potential solvents were considered for the sulfur absorption and stripping process, as shown in Table 2. The H_2S removal process is essentially the same for each solvent, as shown in Figure 1. First, fresh solvent is contacted counter-currently with COG in an absorber where it absorbs the acid gases. Then, the loaded solvent is sent to a stripper, which separates the acid gases from the solvent producing lean solvent in the bottoms which then is recycled to the absorber. Depending on the solvent used, it may be necessary to operate the absorber at a high pressure, thus requiring an additional COG compression step. A small amount of makeup solvent is required to account for any solvent losses through the sweetened COG product and the captured sulfur gases.

Table 2. Comparison of different solvents [22] binary effects with sulfur compounds

Solvent	*Rectisol*	*MDEA*	*MEA*	*DGA*
Solvent type	Physical	Aqueous	Amine	Aqueous amine
Typical Application	Coal to MeOH	IGCC	Commercialized for post-combustion	Commercialized for NG sweeting
Relative volatility (Chemical / Solvent) at 16 bar				
Temperature range (°C)	-60.0 to 150	-70.0 to 410	-80.0 to 300	-70.0 to 370
H_2S	127—5000	458—3.60×10^8	369—6.90×10^7	42.5—7.27×10^4
CS_2	1.93	8.62—33.0	28.9—199	7.87—19.4
C_4H_4S	---	5.58—9.56	20.0—25.5	4.97—6.20
Pressure (bar)				
Absorber	17.0	16.2	1.00	1.00
Stripper	3.40—17.0	2.00	-	1.00

For this work, MDEA was chosen because it had the largest relative volatility with respect to H_2S out of the four solvents considered. Although the high pressure MDEA-based process requires the use of expensive compressors, from a systems perspective this is not a bad choice because the sweetened COG has to be compressed to high pressure anyway for combustion in a gas turbine (GT). Thus, the cost of compression is relatively independent of the choice of solvent. A more comprehensive techno-economic analysis would be needed in order to select the best solvent at the systems level, but this is outside of the scope of the current work. The MDEA selection provides a reasonable and effective base case for use in analysis.

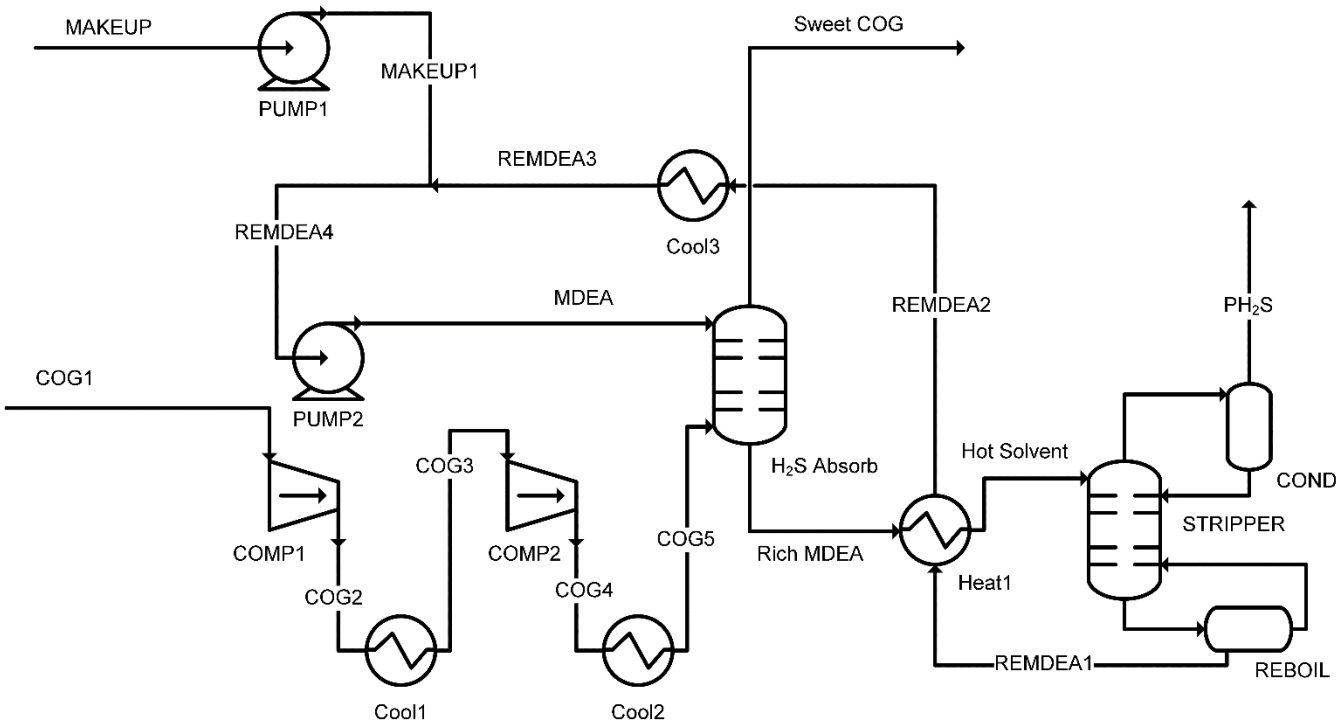

Figure 1. The COG desulphurization process proposed

The process of Figure 1 was simulated in the commercial software package ProMax using the Amines physical properties package. The TSWEET Kinetics column type is used to simulate the absorber and the TSWEET Stripper column process model is used to model the stripper. These models are specifically designed for gas sweeting applications with amines such as MDEA. The design was made using the heuristics suggested by Adams et al. [23] with manual adjustments. Some trial and error was used to estimate the required amount of solvent needed, the number of stages, and the heat required to raise the temperature of the rich solvent before entering the stripper.

2.3. Combined cycle power plant design

The design of the proposed CCPP is shown in Figure 2. The sweet COG (after MDEA desulphurization) is combusted with compressed air at 16.0 bar. Inter-stage coolers are used to ensure that the air temperature does not exceed 250°C in the compressor. The flow rate of air is chosen such that the combustion temperature is 1240°C, which is typical of gas turbine inlet temperatures (for example, Lin et al. [24] reports a value of 1260°C before expansion in the GT). 1240°C was chosen because with the specified GT outlet pressure of 1.7 bar, the predicted GT outlet temperature is just under the HX5 material

temperature limit of 650-700 °C [25]. The GT modeled is based on a 9FA class of GE Power turbine with an isentropic efficiency close to 0.9 [24].

The remaining thermal energy from the exhaust gas is captured through a series of heat exchangers in the bottoming cycle before the exhaust gas is vented to the atmosphere. In the heat exchangers, the gas enters through the shell side, while high pressure steam/water enters through the tube side. The pressure drop is an important factor to be considered. The pressure drop in the shell side for every heat exchanger in the CCPP section is assumed to be 0.1 bar [26]. For the tube sides, the pressure drop is assumed to be 0.3 bar for HX0, 0.4 bar for HX1, 0.8 bar for HX2, 0.8 bar for HX4 and HX5, and 1.2 bar for HX3, based on the recommendations of Gicquel [26]. To make sure that the pressure of the flue gas is high enough to be emitted to open air through a stack without an exhaust fan, the outlet pressure of the GT exhaust is set to 1.7 bar.

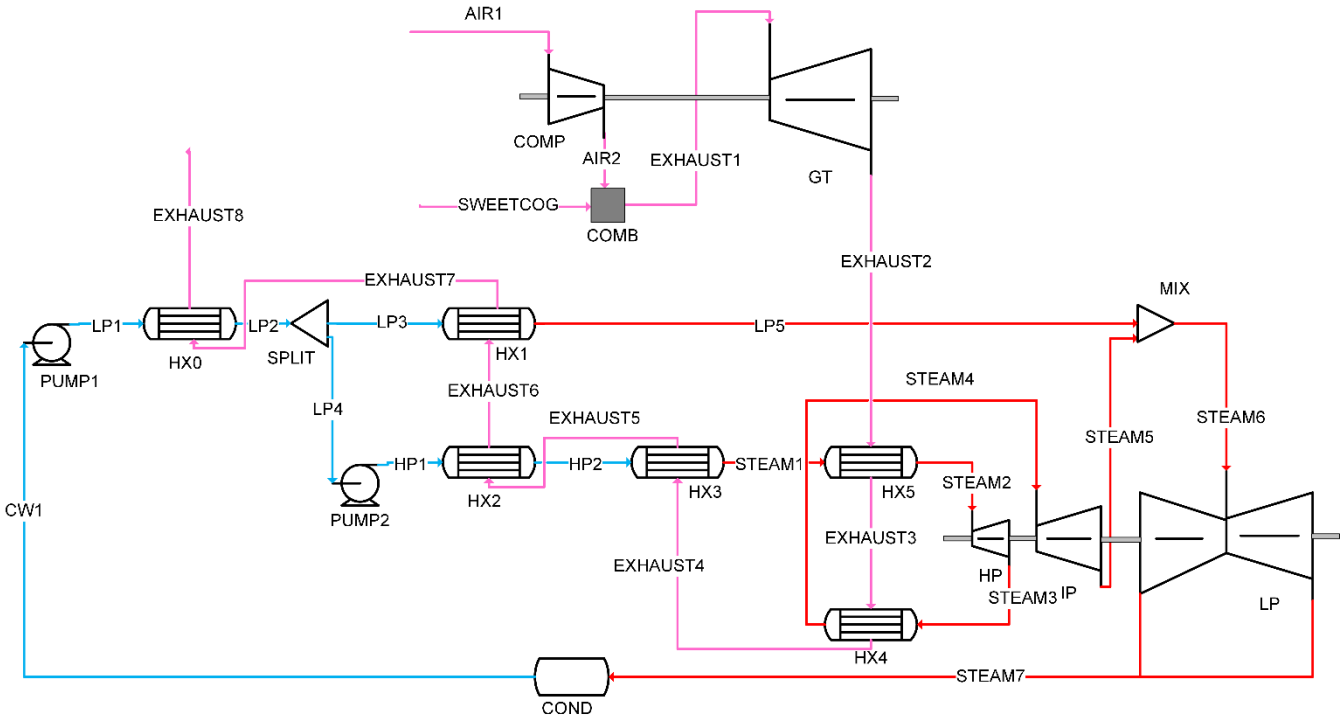

Figure 2. Proposed combined cycle power plant design

The heat transfer coefficient depends on the flow phase conditions in both the shell side and tube side [27]. The heat transfer coefficient is always higher for liquid-liquid than for gas-vapour phase in shell-tube side. For gas phase in shell side and liquid phase in tube side, the heat transfer coefficient without phase change

is in the range between 227-454 W/m^2/K [27]. For vaporization in the tube side, the heat transfer coefficient is much higher, which is more than 1000 W/m^2/K. Details of the assumptions chosen for this work are shown in Table 3.

Table 3. Pressure drop and heat transfer coefficients in heat exchangers

Heat exchangers	Description	Pressure drop (bar)		Heat transfer coefficient (W/m^2/K)
		Shell side	Tube side	
HX0	Gas-liquid HX	0.100	0.300	260
HX1	Vaporization	0.100	0.400	1100
HX2	Gas-liquid HX	0.100	0.800	260
HX3	Vaporization	0.100	1.20	1140
HX4	Gas-Vapor HX	0.100	1.00	140
HX5	Gas-Vapor HX	0.100	1.00	140

Most bottoming processes consist of high pressure (HP), intermediate pressure (IP) and low pressure (LP) steam turbines (ST) when the bottoming cycle has the ability to generate more than 20.0 MW power, and the temperature of the available waste heat from the COG exhaust is high enough to a support steam pressures up to 100 bar [28]. In this study, since total work generated at the bottoming process will exceed 20.0 MW, a three-stage steam turbine system was designed.

In order to recover as much thermal energy as possible, process water is fed to a low pressure heat exchanger. Then it is split into low pressure and high pressure pathways. The low pressure stream goes through a low pressure economizer, and an evaporator. The high pressure stream is pumped to 123 bar and then sent to a high pressure economizer, an evaporator, and a superheater. The HP steam feeds the HP ST. The HP ST exhaust is reheated before being fed to the IP ST. The stream leaving the IP ST is mixed with the LP steam from the LP superheater and fed into the LP ST. The stream leaving of LP ST is condensed and recycled back to the low pressure pump. The isentropic efficiency of the HP, IP, and LP steam turbines are assumed to be 0.88, 0.89, and 0.86 respectively [24].

To model the CCPP in Aspen Plus, the PR-BM thermodynamic property package was used to predict the physical properties of all the gas phase unit operations including the fluid properties on the shell side of the heat exchangers. The STEAMNBS thermodynamic property model was used for all water/steam related unit operations such as the tube side of the heat exchangers in the bottoming cycle. In the Aspen

Plus model, all heat exchangers were modeled using HEATX block, the condenser was modeled with a HEATER block, the combustion step was modelled using RGIBBS assuming equilibrium was reached, and all turbomachinery was modeled using assumed isentropic efficiencies as noted previously.

2.4. Economic analysis of the system

Electricity generated by turbines is the main product of this system. Although the status quo and the CCPP will both emit approximately the same flow rates of GHGs (as measured in CO_2e) in absolute terms, the CCPP results in lower indirect emissions associated with the reduced amount of grid electricity purchased for the balance of the plant (since the AMD refinery consumes more electricity than the CCPP produces). As such, we assume that the value of that reduction in GHG emissions will return to the company in the form of lower CO_2 carbon taxes.

The net present value (NPV) can be formulated as shown in Eq. 1.

$$NPV = AF\ (TR - TOC - TPC) - TCI \quad \text{(Eq. 1)}$$

$$AF = \frac{1-(1+r)^{-t}}{r} \quad \text{(Eq. 2)}$$

where AF represents the annuity factor, TR represents the annual revenue (\$), TOC represents the annual operating cost (\$), TPC represents the total production cost (\$), and TCI represents the total capital investment (\$). For the annuity factor function (Eq.2), r represents the interest rate and t represents the lifetime (yr).

The economic analysis in this work uses a business-case comparison against the status quo in order to quantify the value-added by replacing the existing power system with CCPP. This means that the revenues and production costs used in Eq. 1 are representations of value instead of actual revenues and expenses. For example, the annual value of electricity of the COG CCPP case is the value of the additional net electricity production *over and above* the existing process which produces power at a lower rate from the same amount of COG. This additional net work ($W_{add.}$) is defined in Eq. 3 as follows:

$$W_{add.} = -W_{COMP} + W_{GT} - \sum_{j=1}^{2} W_{PUMP,j} + \sum_{k=LP,IP,HP} W_{ST,k} - W_{current} \quad \text{(Eq. 3)}$$

where W_{COMP}, $W_{PUMP,j}$, W_{GT}, $W_{ST,k}$, and $W_{current}$ represent work (kW) consumed by compressor and pumps, work generated by gas turbine and steam turbine, and the net work currently produced using the

status quo system, respectively. The value for $W_{current}$ was provided for this case study by AMD Hamilton but is not disclosed for privacy reasons. This value-added electricity is priced at grid electricity purchase prices including delivery (not wholesale prices) because the primary value of the CCPP is to offset AMD Hamilton's grid electricity purchases, which far exceed the power produced by the COG CCPP. Similarly, under a carbon tax, there is value in the reduction of GHG emissions priced at the carbon tax rate. Although the actual GHG emissions will be reduced indirectly (through reduced grid electricity generation), it is assumed that value of the reduction in emissions in a fair system will be ultimately returned to AMD. Assuming 8000 annual working hours per year, the annual revenue becomes:

$$TR = 8000 hr/yr \; W_{add.} \left(x_{elec.} + R_{CO_2} \right) \quad \text{(Eq. 4)}$$

$$R_{CO_2} = \omega_{CO_2} \; Tax_{CO_2} \quad \text{(Eq. 5)}$$

where $x_{elec.}$ represents the price of electricity (\$/kWh), R_{CO_2} represents the revenue from carbon tax (\$/kWh). ω_{CO_2} represents the carbon intensity of the electrical grid (tCO_2e/kWh), and Tax_{CO_2} represent the tax of CO_2 (\$/tCO_2e). In this study, these parameters are assumed to be constant during the lifetime of the process.

The annual operating costs include COG consumption, MDEA makeup solvent costs, and utility costs. The makeup water flowrate is computed, but the costs of makeup water is assumed to be zero. Although other studies assumed prices for COG based on heating content [29], it is not appropriate to use a value of COG for our case study. This is because we consider the difference in value between the status quo and the proposed COG CCPP use case. Since it has the same value in both cases (i.e. a waste product with a very limited market), the value added (or extra cost) is zero and so it does not appear in the equation for the production costs. Thus, the annual operating costs include only the extra costs associated with the purchase of makeup MDEA and utility costs over and above the utility water requirements of the status quo:

$$TOC = 8000 \frac{hr}{yr} \left(x_{MDEA} \, m_{MDEA,makeup} + x_{cond} \, Q_{cond} + x_{reb} \, Q_{reb} + x_{CW} \left(Q_{comp} + Q_{cool,MDEA} + Q_{CCPP} - Q_{SQ} \right) \right) \quad \text{(Eq. 6)}$$

where x_{MDEA} represents the price of MDEA (\$/kg), $m_{MDEA,makeup}$ represents the flow rate of makeup MDEA (kg/hr), x_{cond} and x_{reb} represent the prices of the condenser and reboiler utilities (\$/GJ) in the desulphurization section, respectively, Q_{cond} and Q_{reb} represent the duties of the condenser and reboiler utilities (GJ/hr) in the desulphurization section, respectively, x_{CW} is the price of cooling water (\$/GJ),

Q_{comp} represents the total inter-stage cooling duty of the COG and air compressor, $Q_{cool,MDEA}$ represents the cooling duty of recycling MDEA solvent in desulphurization process, and Q_{CCPP} and Q_{SQ} are the total condenser duties (GJ/hr) of the steam sections of the COG CCPP and status quo plants, respectively.

The total annual production cost is defined in the Appendix Table A.1. The TPC ($/yr) is calculated according to Seider et al.'s book, page 604 [27]. It includes operations (labour-related), maintenance cost, operating overhead, property taxes and insurance, depreciation, and general expenses. Note that for this analysis, we assume that the TPC of the status quo is zero, due to the lack of publically available data for the TPC of the existing system at the AMD Hamilton refinery. Thus, this serves as a very conservative estimate of the value of the COG CCPP system. In other words, a strong business case would be made for the CCPP system if the NPV and other economic criteria are favourable even with this assumption. Q_{SQ} is estimated according to the size of the status quo. It is assumed that the pressure inlet and outlet of the LP ST in both the status quo and the COG CCPP are the same. Thus the heat duty (Q_{SQ}) is linearly regressed with respect to the amount of work generated in the LP ST.

The equipment required in this new CCPP includes a compressor, a combustor, a gas turbine, two pumps, six heat exchangers, three steam turbines, and the equipment of the whole desulphurization process. Thus the total free-on-board (F.O.B.) cost (C_{fob}) is calculated as Eq.7:

$$C_{fob} = C_{COMP} + C_{COMB} + C_{GT} + \sum_1^2 C_{PUMP,j} + \sum_1^2 C_{motor,j} + \sum_0^5 C_{HX,i} + \sum_k C_{ST,k} + C_{MDEA} \qquad \text{(Eq. 7)}$$

where $C_{COMP}, C_{COMB}, C_{GT}, C_{PUMP,j}, C_{motor,j}, C_{HX,i}, C_{ST,k}, C_{MDEA}$ represent the F.O.B cost of the compressor, combustor, gas turbine, pumps, pump motors, heat exchangers, steam turbines and desulphurization process, respectively.

The equipment free on board (F.O.B.) cost of topping cycle equipment is based on 1982 prices [30] while the bottom cycle equipment is based on 2006 prices [27]. To convert the cost to present cost, the Chemical Engineering Plant Cost Index (CEPCI) [31] for 2016 is used. For this research, these F.O.B. costs are converted to 2016 CAD with the following equation.

$$PRESENT\ COST = BASE\ COST\ \frac{CEPCI_{new}}{CEPCI_{old}}\ PPP \qquad \text{(Eq. 8)}$$

where PPP is the purchasing power parity of Canada [32] relative to that of the United States in this case since the cited equipment cost curves are for US applications. Also, we note that the topping cycle

equipment cost projections, although old, are the most recent we could find in the peer-reviewed literature and continue to be used in recent studies [30]. However, an online database of user-supplied actual purchase prices indicated that the cost for a similar topping cycle equipment at a similar scale was around $10 million for the equipment purchase costs [33]. Although we did not use this price because it is not verifiable or peer reviewed, when the cost of installation (including shipping, piping, etc.) using assumed capital investment factor by Seider et al. [27] is considered, the total installed cost would be in the range of $30-60 million. The installed cost predicted using the peer-reviewed correlations and the CEPCI is within this range and therefore is a reasonable estimate for this analysis.

The total capital investment (TCI) includes the F.O.B. costs and any related costs such as shipping, installation, construction, construction overhead, contractor engineering, contingencies, depreciation, land, royalties, start-up, and total working capital. A detailed calculation of the TCI is shown in Appendix Table A.2 [27].

The compressor cost (C_{COMP}) is correlated to the mass flow rate of air (m_{air}: kg/hr), its compression efficiency (η_{comp}), outlet to inlet pressure ratio, and number of compression stages (N) [30]:

$$C_{COMP} = \left(\frac{1}{N}\right)\left(0.01975\ \frac{m_{air}}{0.9-\eta_{comp}}\right)\left(\left(\frac{P_{air}^{out}}{P_{air}^{in}}\right)^{\frac{1}{N}}\right)\left(ln\left(\frac{P_{air}^{out}}{P_{air}^{in}}\right)\right) \qquad \text{(Eq. 9)}$$

The cost of the combustor (C_{COMB}) is correlated to mass flow rate of air, outlet ($\mathrm{P}_{\mathrm{g,COMB}}^{\mathrm{out}}$) to inlet ($\mathrm{P}_{\mathrm{air}}^{\mathrm{in}}$) pressure ratio, and outlet temperature ($\mathrm{T}_{\mathrm{g,COMB}}^{\mathrm{out}}$) [30].

$$C_{COMB} = \left(0.0128\ \frac{m_{air}}{0.995-\frac{P_{g,comb}^{out}}{P_{air,comb}^{in}}}\right)\left(1+e^{\left(0.018\,T_{g,COMB}^{out}-26.4\right)}\right) \qquad \text{(Eq. 10)}$$

The cost of the gas turbine (C_{GT}) is correlated to mass flow rate of gas ($\mathrm{m_g}$: kg/ hr), and is affected by inlet to outlet pressure ratio, inlet temperature ($\mathrm{T}_{\mathrm{g}}^{\mathrm{in}}$), and efficiency of the turbine (η_{GT}) [30]:

$$C_{GT} = 0.13315\ \left(\frac{m_g}{0.92-\eta_{GT}}\right)\left(ln\left(\frac{P_g^{in}}{P_g^{out}}\right)\right)\left(1+e^{\left(0.036\,T_g^{in}-54.4\right)}\right) \qquad \text{(Eq. 11)}$$

The F.O.B. cost of pumps $C_{PUMP,j}$ is correlated to pump type $\left(\mathrm{F_{t,pump}}\right)$, material type$\left(\mathrm{F_{m,pump}}\right)$, and the base cost of that pump$\left(\mathrm{C}_{B,PUMP,j}\right)$. Considering the large amount of water to be pumped, a centrifugal pump is chosen in this paper [27].

$$C_{PUMP,j} = F_{t,pump}\, F_{m,pump}\; C_{B,PUMP,j} \qquad \text{(Eq. 12)}$$

The base cost of the pump as calculated by Eq.13 is correlated to shape factor (S) [27], while the shape factor is a function of water flow rate (V) in gallons/minute, and pump head (H) in feet.

$$C_{B,PUMP,j} = e^{(9.7171 - 0.6019\ ln(S_j) + 0.0519\ (ln(S_j))^2)} \qquad \text{(Eq. 13)}$$

$$S = V * (H)^{0.5}, S \in [400, 1E5] \qquad \text{(Eq. 14)}$$

A centrifugal pump is usually driven by an electric motor. Depending on which type of motor used, the motor-type factor ($F_{t,motor,j}$) will apply. The cost of an electric motor is a function of the horsepower consumption ($HP_{pump,j}$) [27]:

$$C_{motor,j} = F_{t,motor,j}\, e^{(5.8259 + 0.13141\, ln(HP_{pump,j}) + 0.053255\, (ln(HP_{pump,j}))^2 + 0.028628\, (ln(HP_{pump,j}))^3 - 0.0035549\, (ln(HP_{pump,j}))^4)}$$

(Eq. 15)

The electricity needed for the pump is factored into the net output of the CCPP.

A fixed head type heat exchanger is chosen in this work [27]. Which the base cost $(C_{B,HX,i})$ of a heat exchanger is a function of heat exchange area A_i.

$$C_{B,HX,i} = e^{(11.2927 - 0.9228\ ln(A_i) + 0.09861\ (ln(A_i))^2)} \qquad \text{(Eq. 16)}$$

The free on board (F.O.B) cost of heat exchanger ($C_{HX,i}$) is correlated to the material type$(F_{m,HX})$, length of the tube$(F_{L,HX})$, the shell side pressure factor$(F_{p,HX})$, and the base cost$(C_{B,HX,i})$.

$$C_{HX,i} = F_m\, F_L\, F_p\; C_{B,HX,i} \qquad \text{(Eq. 17)}$$

The pressure factor is a function of pressure (in psig) in shell side as shown in following equation, which is applicable from 100 to 2,000 psig:

$$F_p = 0.9803 + 0.018\ \frac{P}{100} + 0.0017\ \left(\frac{P}{100}\right)^2 \qquad \text{(Eq. 18)}$$

HP and IP steam turbines are noncondensing while LP stream turbine is condensing type. In addition, the size of LP steam turbine is larger than normal steam turbine, two parallel LP ST are used. The F.O.B. purchase cost of the steam turbine is shown in the following equation from Seider et al, page 591 [27].

$$\left.\begin{array}{l} C_{ST,k} = 9400\ (W_{ST,k}/0.7355)^{0.41}, k = HP, IP \\ C_{ST,k} = 50000\ (W_{ST,k}/1.471)^{0.41}, k = LP \end{array}\right\} \qquad \text{(Eq. 19)}$$

To build a new plant, the payback period is a crucial criterion. As Eq. 20 shows, the payback period (y) is calculated using a shortcut approach:

$$y = \frac{TCI}{TR - TOC - TPC} \qquad \text{(Eq. 20)}$$

2.5. Optimization of the system

An optimization approach was used to determine the design parameters for the CCPP. Although the ProMax and AspenPlus simulations are useful for rigorous performance and stream output predictions, they are not directly amenable to rigorous global optimization due to their complexity. Instead, a simplified model of the chemical plant was used in a mathematical programming framework to determine the optimal plant design. The rigorous ProMax and Aspen Plus models were used for the creation of certain reduced models as well as for the validation of the optimization results.

The CCPP system design has certain fixed conditions such as some of the steam turbine pressures and temperature are shown in Table 4.

Table 4. Specified stream conditions based on the optimization of [28]

Component	Temperature Inlet (°C)	Pressure Inlet (bar)	Temperature Outlet (°C)	Pressure Outlet (bar)
GT	1240	16.0	692	1.70
HP ST	540	120	318	25.0
IP ST	540	24.0	302	4.00
LP ST	339	4.00	51.0	0.130

The key decision variables are the surface area of each heat exchanger A_i, the process water flow rate (m_{H_2O}), and the split fraction ($1-\gamma$) of the process water going to the LP steam turbine. The optimization formulation is shown in the following equations.

$$\underset{A_i, m_{H_2O}, \gamma}{maximize} \quad NPV\,(A_i, m_{H_2O}, \gamma) \qquad \text{(Eq. 21)}$$

Subject to:

$$\left.\begin{array}{l} m_g\left(h_{g,i}^{in} - h_{g,i}^{out}\right) - m_{H_2O}\left(h_{H_2O,i}^{out} - h_{H_2O,i}^{in}\right) = 0, i = 0 \\ m_g\left(h_{g,i}^{in} - h_{g,i}^{out}\right) - \gamma\, m_{H_2O}\left(h_{H_2O,i}^{out} - h_{H_2O,i}^{in}\right) = 0, i = 2-5 \\ m_g\left(h_{g,i}^{in} - h_{g,i}^{out}\right) - (1-\gamma)\, m_{H_2O}\left(h_{H_2O,i}^{out} - h_{H_2O,i}^{in}\right) = 0, i = 1 \end{array}\right\} \qquad \text{(Eq. 22)}$$

$$m_g\left(h_{g,i}^{in}-h_{g,i}^{out}\right)-U_i\,A_i\,\Delta T_{LM,i}\;=0,\;A_i\in[14.0,1120],i=0\;to\;5 \quad \text{(Eq. 23)}$$

$$m_{H_2O}\left(h_{cond,ccpp}^{out}-h_{cond,ccpp}^{in}\right)-\;Q_{cond,ccpp}=0 \quad \text{(Eq. 24)}$$

$$\Delta T_{LM,i}-\frac{\left(T_{g,i}^{in}-T_{H_2O,i}^{out}\right)-\left(T_{g,i}^{out}-T_{H_2O,i}^{in}\right)}{ln\left(\frac{T_{g,i}^{in}-T_{H_2O,i}^{out}}{T_{g,i}^{out}-T_{H_2O,i}^{in}}\right)}=0,\;i=0\;to\;5 \quad \text{(Eq. 25)}$$

$$h_l-(a_l\,T_l-b_l)=0 \quad \text{(Eq. 26)}$$

$$h_{mix}-\left((1-\gamma)\,h_{LP}+\gamma\,h_{IP}\right)=0 \quad \text{(Eq. 27)}$$

$$\left.\begin{array}{l}W_{pump,j}-m_{H_2O,j}\left(h_{H_2O,j}^{out}-h_{H_2O,j}^{in}\right)=0,j=1\\ W_{pump,j}-\gamma\,m_{H_2O,j}\left(h_{H_2O,j}^{out}-h_{H_2O,j}^{in}\right)=0,j=2\end{array}\right\} \quad \text{(Eq. 28)}$$

$$\left.\begin{array}{l}W_{ST,k}-\gamma\,m_{H_2O,k}\left(h_{H_2O,k}^{out}-h_{H_2O,k}^{in}\right)=0\,,k=HP,IP\\ W_{ST,k}-m_{H_2O,k}\left(h_{H_2O,k}^{out}-h_{H_2O,k}^{in}\right)=0\,,k=\;LP\end{array}\right\} \quad \text{(Eq. 29)}$$

$$\left.\begin{array}{l}T_{g,i}^{out}-\;T_{g,i}^{in}<0\\ T_{H_2O,i}^{in}-T_{H_2O,i}^{out}<0\\ T_{H_2O,i}^{out}-T_{g,i}^{in}<0\\ T_{H_2O,i}^{in}-T_{g,i}^{out}<0\end{array},i=0\;to\;5\right\} \quad \text{(Eq. 30)}$$

where h represents the enthalpy of a process liquid and gas in J/kg, subscripts H_2O, g, l, mix, IP, and LP represent water or steam streams, gas streams, set of streams whose enthalpy are linear modeled, stream after the MIX block, and intermediate pressure and low pressure streams before the MIX block, respectively. Superscripts out and in denotes output and input of heat exchanger. The heat transfer coefficient (U_i) is constant as shown in Table 3. $\Delta T_{LM,i}$ represents the log mean temperature difference of each heat exchanger, which is the driving force of each heat exchanger. T represents temperature in °C, and a and b represent constants of the linear regression model for enthalpy. Notice that for each stream in the bottoming cycle as shown in Figure 2, the pressure of each stream is fixed. If the temperature is not specified, a linear model is used to estimate the enthalpy of that stream. Thus, the enthalpy of each stream can be represented by Eq. 26. For those streams with specified temperature, the enthalpy is constant.

Eq.22 to Eq.29 are the equality constraints of the optimization problem. Eq.22 is the energy balance between shell side and tube side. Eq.23 is the energy balance of the heat exchanger with heat exchange area bounded in a given range [14.0, 1120] m^2. Eq.24 is the energy balance of condenser in CCPP. The thermal energy decreasing in recycled process water is the amount that the condenser removed. Eq.25 is the heat exchanger driving force. The coefficients in Eq.26 and Eq.27 are determined by linear regression of the STEAMNBS model in Aspen Plus over the relevant temperature range with a good fit (R^2 greater than 0.99).

The flow rate of COG, the GT inlet temperature, and GT inlet pressure are set as a fixed value according to design requirement as mentioned in the Table 4. The net work generated in the topping process is fixed. Thus the work of compressor and GT is a known constant value. For pumps and steam turbines, the working fluid is water/steam. Thermal energy is converted to mechanical energy. The work consumed by pump ($W_{pump,j}$) and work generated by steam turbines ($W_{ST,k}$) could be calculated in the form of enthalpy change. Thus the work is calculated in the Eq.28-29.

Eq.30 ensures that there is no temperature crossover in each heat exchanger. Setting a minimum approach temperature (or pinch point) is not necessary because small approach temperatures (which would result in extremely high heat exchanger areas) are automatically avoided because of the economic objective. Most variables were left unbounded except for the temperature of the flue gas exhaust (EXHAUST8) which had a lower safety bound of 75°C,

The above simplified model of the CCPP was constructed in the General Algebraic Modelling System (GAMS version 24.7.4. IPOPT (version 3.12) and CONOPT (version 3.17A) were used to find local optima that were used as initial guesses for BARON (version 16.8.24), which later found the global optimum. There were 80 variables in total, 63 variables with only lower bounds, 9 variables with lower and upper bounds, and zero variables with only upper bounds. The total number of equality constraints is 78 and total number of inequality constraints is 17. The total CPU time for IPOPT function evaluations was around 0.1 seconds, with the total CPU time for BARON once initialized with that result was around 0.002 sec.

3. Results and discussion

3.1. Desulphurization results

The key design parameters and ProMax simulation results are shown in Table 5. Two-stage of compressors were used. The second compressor consumed 8% more power than the first compressor. The makeup water flow rate is about 1.10% of the flow rate of the bulk solvent requirement. The makeup MDEA flow rate is very low, which means that there is very little solvent loss in the desulphurization process. The desulphurization process achieved 99.8% of H_2S removal, while little of the organic sulfur compound CS_2 and thiophene (C_4H_4S) were removed as expected. However, the H_2S content in the sweet COG is less than 1.00 PPMV, meaning that the total sulfur content is low enough to use in the gas turbine, despite the presence of CS_2 and thiophene.

Table 5. Design parameters and simulation results for the MDEA process

Compression			
Compressor 1 outlet pressure (bar)	5.00	Comp 1 work (MJ/kg COG)	0.370
Compressor 2 outlet pressure (bar)	16.2	Comp 2 work (MJ/kg COG)	0.400
Absorber			
Gas inlet temperature (°C)	46.6	Sweet COG H_2S Content (ppmv)	0.100
Solvent inlet temperature (°C)	46.6	Sweet COG CS_2 Content (ppmv)	80.2
Solvent rate (kg solvent/kg COG)	1.77	Sweet COG C_4H_4S Content (ppmv)	25.5
Number of stages	18.0		
Stripper			
Number of stages	8.00	H_2S recovery (1-kg H_2S in product/kg H_2S in feed)	99.8%
CS_2 recovery (1-kg CS_2 in product/kg CS_2 in feed)	0.460%	C_4H_4S Recovery (1-kg C_4H_4S in product/kg C_4H_4S in feed)	5.36%
Reflux ratio	10.0	Boilup ratio	3.44
Cooling duty (MJ/kg feed)	2.17	Heat duty (MJ/kg feed)	0.570
Distillate temperature (°C)	40.0	Bottoms outlet temperature (°C)	210
Makeup			
Water makeup/losses (kg H_2O added per kg H_2O in solvent absorber feed)	0.011	MDEA makeup/losses (kg MDEA added per kg MDEA in solvent absorber feed)	7.80×10^{-6}

3.2. GAMS model match with Aspen Plus

The parameters that were used to calculate the capital cost of the system are shown in Table 6. The pressure in the shell side of the heat exchanger drops from 1.70 to 1.10 bar (30.7 to 39.4 psig). According to Eq. 18, the pressure factor (F_p) for the heat exchanger is range from 0.986-0.988, thus approximate to 0.988 for all cases instead of having an equation for calculating F_p in GAMS. The longest standard tube length is 20.0 ft (6.10 m), which in this paper was chosen for heat exchanger calculations considering the area of each heat exchanger was in the order of 1000 m^2. For the pump impeller, cast iron is inferior to bronze in corrosion, erosion and cavitation resistance. Stainless steel impellers have the highest resistance of corrosion, erosion, and cavitation, but it is more costly. Thus bronze material is chosen for both the impeller and the casing [34]. There are three types of electric motor that could be used for the pump: open, drip-proof enclosure, size range from 1 to 700 Hp; totally enclosed, fan-cooled, size range from 1 to 250

Hp; and explosion-proof enclosure, size range from 1 to 250 Hp. The pump is used to pump water, which is relatively safe and has no large temperature increase, thus an open, drip-proof enclosure type is chosen.

For the utility costs, 450 psig steam (235.8°C) was chosen for the desulphurization reboiler utility. The HRSG condenser, distillation condenser, and inter-stage coolers for compressors all use cooling water (assuming an operating temperature range of 32 to 49°C). The corresponding price of utilities is shown in Table 6, based on [27].

Table 6. Parameters used in the base case calculation

Parameters	Description	Value	Parameters	Description	Value
$F_{m,\ HX}$	Carbon steel	1.00	$F_{t,\ PUMP}$	centrifugal	8.90
F_p	1.7 (bar)	0.981	$F_{t,\ motor}$	Open, drip-proof enclosure, 1 to 700 Hp	1
Fl	20 (ft)	1.00	x_{cond} & x_{cw}	Price of cooling water (US $/GJ)	0.048
$F_{m,\ PUMP}$	bronze	1.90	x_{reb}	Price of steam at 450 psig (US $/GJ)	8.13

The base case uses Ontario's global adjusted electricity price (11.2 ¢/kwh) [35], an interest rate of 15.0%, a lifetime of 30 years, Ontario's electricity grid carbon intensity of 40 $gCO_2eq./kWh$ [36], and Ontario's average carbon tax in 2017, which is $18.1/tonne [37]. Although the current carbon tax system in Ontario includes a complex arrangement of emissions credits, we assume that all of the associated CO_2 emissions are taxable. To validate the reduced model used in GAMS, the optimal decision variables determined by GAMS were used as inputs to the Aspen Plus simulation, and the Aspen Plus results of key variables were compared, as shown in Table 7.

Table 7. The results of the optimization model (using simplified models), and the corresponding results of key variables when the design was simulated more rigorously in Aspen Plus. Results are for the base case.

Component	*Description*	*GAMS*	*Aspen Plus*	*Error (%)*
m_{air}	kg air/kg COG	28.5	28.5	0.00
m_{H_2O}	kg water circulated in bottoming process/kg COG	6.56	6.56	0.00
T_g^1	Temperature of EXHAUST1 (°C)	1240	1240	0.00
T_g^2	Temperature of EXHAUST2 (°C)	692	692	0.00

T_g^3	Temperature of EXHAUST3 (°C)	634	634	-0.01
T_g^4	Temperature of EXHAUST4 (°C)	599	599	-0.02
T_g^5	Temperature of EXHAUST5 (°C)	510	511	-0.04
T_g^6	Temperature of EXHAUST6 (°C)	445	446	-0.15
T_g^7	Temperature of EXHAUST7 (°C)	191	190	0.41
T_g^8	Temperature of EXHAUST8 (°C)	98.0	96.0	1.51
$T_{H_2O,vap.}^6$	Temperature of STEAM6 (°C)	206	205	0.32
$T_{H_2O,vap.}^7$	Temperature of STEAM7 (°C)	51.1	51.1	0.01
Total Power Generated	MJ/kg COG	25.9	25.9	0
Total Net Work	MJ/kg COG	13.3	13.3	0
Total HX. Area	Total HX. Area (m^2)	2150	2180	-1.15
Topping Net Work	MJ/kg COG	7.93	7.93	0
Bottoming Net Work	MJ/kg COG	5.40	5.38	0.37

The temperature of the EXHAUST streams and two adjustable steam/water streams have a small error. The biggest error is the temperature of stream EXHAUST8, which is the stack temperature. But all the errors are less than 1.51%, which is small. Thus the result from GAMS optimization is reasonable, and the simplified GAMS model is good for further use with other parameters.

As table 7 shows, every 1 kg of COG will need 6.56 kg water in order to achieve highest NPV for the CCPP. The total gross power generated is about 25.9 MJ/kg COG, while the total net work is 13.3 MJ/kg COG.

3.3. Economic analysis

For the base case, the topping cycle generates about 59.5% of the total work, while the bottoming cycle generates 40.5% of electricity as shown in Table 8. According to M. Boyce [28], the topping cycles of combustion systems usually generate around 60.0% of the power, which is very much in line with our results. The thermal efficiency of CCPP from natural gas can be as high as 60.0% when the outlet pressure of gas from GT is at atmospheric pressure as M. Boyce, et al. stated [28]. In this case, however, the thermal efficiency is about 34.7% because the HHV of COG is only about half that of natural gas. However, the

proposed CCPP has more than twice the efficiency (15.0% high heating value) of AMD Hamilton's existing COG combustion power system.

Table 8. Economic analysis of proposed COG CCPP compared with status quo

	Proposed COG CCPP				**Business As Usual/Status quo**
	Desulphurization	Topping	Bottoming	**Total**	
MJ/kg COG	-	7.93	5.4	**13.3**	**5.77**
TCI (million $)	1.29	50.0	17.2	**68.5**	**0**
TOC ($/kW)	-	-	-	**31.4**	**0**
TPC ($/kW)	-	-	-	**288**	**0**
TR ($/kW)	-	-	-	**512**	**0**
Payback period (yr)	-	-	-	**5.77**	**0**
NPV(million $)	-	-	-	**9.51**	**0**
Installation cost ($/kW)	-	1359	685	**1107**	**0**

The installation cost of the topping process is about 3 times of the bottoming process. The high cost of the topping cycle might be the reason why a considerable number of steel refineries only use low pressure steam turbines even though they have lower energy recovery. The total installation cost of this proposed system is 1107 $/kW, which is higher than the common CCPP plant whose cost range falls between 600 and 900 $/kW [28]. However, this includes the desulfurization cost, which comprises 1.9% of the total cost. Without the desulfurization process taken into account, the CCPP installation cost would only be 1086 $/kW. The NPV of the business as usual scenario evaluates to $0 million according to Eq.1. Thus, the CCPP plant is a good risk for an investment because it has a potential net present value of $9.51 million (including the benefits of reduced grid electricity purchases and reduced carbon taxes), within 6 years (payback period of 5.77 yr) and only $68.5 million in capital investment. In addition, the net lifecycle CO_2 emissions reduced is 84.1 gCO_2e/kg COG with the local carbon intensity of 40 gCO_2e/kWh. This represents a net lifecycle reduction in GHG emissions arising from COG combustion by about 5.28%. However, the direct CO_2 emission of AMD status quo is 995 gCO_2e/kWh, while the proposed CCPP reduces it to 430 gCO_2e/kWh.

3.4. Sensitivity analysis of the system

Considering that the electricity price, carbon intensity, carbon tax, PPP, and annuity factor might change according to government policies and market effects, business case for using the proposed system may

change accordingly. Thus the uncertainty of the above mentioned five factors are considered in a sensitivity analysis. The worldwide electricity price ranges from [3.00, 60.0] CAD ¢/kWh [38-40]. However, Grid carbon intensity ranges from [2.05, 4553] gCO_2 eq./kWh. The carbon tax rate ranges from [0.00, 70.0] CAD $/tonne [37, 41]. Carbon tax revenue R_{CO_2} thus ranges from [0.00, 0.319] CAD $/kWh. And for the annuity factor, assuming that the interest rate range is [10.0%, 50.0%] and the lifetime range is [10.0, 50.0] years, the AF is in the range of [1.70, 10.0]. However, it is usually the case that countries with very high carbon intensity have little or no carbon tax. Also, when the carbon intensity is high, the PPP is high as well, which means the cost of applying this proposed COG CCPP is high. The optimization problem was resolved using 10 points generated by Latin hypercube in the above ranges. The global optimal design, however, was the same for all cases. The NPV is a function of electricity price, carbon tax rate, PPP, and annuity factor as Eq.31 shows.

$$NPV = AF\left(\left(248.558\left(x_{elec.}\frac{1\$}{100¢} + R_{CO_2}\right) - PPP\ (\$1.532)\ -\ \$14.2\right) - PPP\ (\$54.003)\right) \times 10^6 \quad \text{(Eq. 31)}$$

As the electricity price and carbon tax rate increases, the NPV increases. When the interest rate is 15.0%, lifetime is 30 years (meaning when AF is 6.57), and there is no carbon tax credit (which means that carbon tax rate is zero), the electricity price could be as low as 10.8 CAD ¢/kwh to still have a positive NPV. If the price is lower than that, the CCPP is not recommended.

The payback period within the above range is given as Eq.32.

$$y = \frac{\$54.003\ PPP}{248.55788\left(x_{elec.}\frac{1\$}{100\,¢} + R_{CO_2}\right) - \$\,1.532\ PPP - \$14.2} \quad \text{(Eq. 32)}$$

For the base case, payback period is about 5 years. When the electricity price goes up to above 15.1 ¢/kwh, or R_{CO_2} goes above 0.157 $/kWh, the payback period will be reduced to 3 years.

Four other representative locations are chosen as case study. Which are China, USA, Finland, and Mexico, each of them have different electricity price, carbon tax, carbon intensity of their electric grid, and PPP. Notice that the carbon intensity for USA, Finland, Mexico and China are calculated as follows:

$$\omega_{CO_2} = \frac{CO_2\ emissions\ from\ electricity\ and\ heat\ production(\%\ of\ total\ fuel\ comb.) \times total\ CO_2\ emission\ (kt)}{electric\ power\ consumption\left(\frac{kWh}{capital}\right) \times total\ population} \quad \text{(Eq. 33)}$$

The data used to calculate carbon intensity in Eq. 33 are from the World Bank, 2016 [42-45]. Table 9 is the comparison between those cases as well as the AMD case.

Table 9. Economic analysis of COG CCPP applied in various locations assuming AF=6.57.

	Ontario, Canada	USA	Finland	Mexico	China	Units	Ref.
PPP	1.27	1	0.905	8.57	3.47	LCU/USD	[32]
ω_{CO_2}	40	588	285	856	1064	g/kWh	[42-45]
Tax_{CO_2}	18.1	0	29.3	3.70	0	$/tonne	[37, 41, 46]
$x_{elec.}$[a]	0.112	0.108	0.175	3.65	0.660	LCU/kwh	[47-49]
NPV	13.8	19.5	164	286	115	Million USD	
Y	5.18	4.82	1.63	0.53	1.30	yr	

[a]: LCU = local currency unit (Canada in CAD, USA in USD, Finland in Euro, Mexico in MXN, and China in RMB).

For the five cases shown in Table 9, they are based on AF= 6.57. Even though Finland has very low carbon intensity (285 $gCO_2e./kWh$), it has very high carbon tax (29.32 $/tonne) [41]. While for Mexico, its carbon intensity (856 gCO_2e/kWh) is about three times that of Finland, but its carbon tax is low (3.7 $/tonne) [42]. For the USA case, even though its R_{CO_2} is zero, its capital cost is lower compared to the AMD, Canada case, and thus there is an even stronger business case for using COG CCP in the USA. For Mexico and China, not only are the economic gains large, but indirect CO_2 emissions can be reduced by 241 $ktCO_2e/yr$ and 299 $ktCO_2e/yr$ respectively with the same COG flow rate per instance. As of 2016, China produced 808.4 Mt of crude steel [50]. If China applied this proposed COG CCPP, and assuming a COG production rate of the total CO_2 emission reduced would be 53.7 $MtCO_2e/yr$. For the whole world, the CO_2 emission reduction would be 108 $MtCO_2e/yr$.

The cost of CO_2 avoided (CCA) in this proposed COG CCPP is the extra costs of doing a "green" technology compared to a status quo, divided by the reduction in emissions as a result of that technology. This means that:

$$CCA = \frac{NPV_{SQ} - NPV_{CCPP}}{30yr\ (8000\ hr\ \omega_{CO_2} W_{add.})} \qquad \text{(Eq. 34)}$$

where $NPV_{SQ}$and NPV_{CCPP} represent the net present value of the status quo and proposed COG CCPP. The NPV calculated in Eq.34 are without revenue from carbon tax. The CCA for Canada and China is -2.21 and -12.8 $/$tCO_2e$, respectively.

4. Conclusion

This paper proposed a design and examined the economics of a COG based fuel CCPP process. It was found that if the current steam power plant were replaced with the proposed CCPP, it could achieve $8.34 million in net present value under base case market conditions. The payback period is also relatively short. The potential environmental benefit for this particular case study, however, is relatively small, because the reduction in GHG emissions is associated with avoided electricity purchases from an electric grid which already has a low carbon intensity. But the impact of using this same technology in other markets is substantially different.

A sensitivity analysis was conducted that yielded a simple bi-linear prediction of the NPV of this investment as a function of the annuity factor (easily computed from project lifetime and interest return rates), price of electricity, and the value of avoided carbon taxes (easily computed from grid carbon intensity and carbon taxes). However, this analysis does not include important case-specific factors such as the lost productivity due to lost electric power produced by the status quo system during the retrofit construction period, which would add to the cost. This also does not reflect the additional cost of other practical issues during this retrofit construction period such as having to add in more substations/transition lines to provide for lost power from the grid during retrofit so the rest of the refinery can still operate.

In future work, we consider alternative COG disposal strategies, such as conversion to methanol or H_2. The potential advantages would be significantly lower direct grid CO_2 emissions from the plant and the displacement of fossil-based primary energy products (such as petroleum-derived methanol). However, this would be offset by increased grid electricity consumption, CO_2 emissions associated with indirect emissions of downstream product use, and the adoption of business activity which is a typical for a steel refinery, such as liquid/gaseous chemical production and CO_2 sequestration. The CCPP approach presented in this study will serve as an important benchmark for comparative purposes.

Acknowledgements

This invited contribution is part of the I&EC Research special issue for the 2018 Class of Influential Researchers. Helpful collaborations and data from Ian Shaw and David Meredith (AMD) are gratefully acknowledged. This research was funded by the McMaster Advanced Control Consortium, of which AMD is a member.

Nomenclature

Abbreviations

AMD	ArcelorMittal Dofasco
BFG	blast furnace gas
BOFG	basic oxygen furnace gas
CEPCI	chemical engineering plant cost index
CO_2e	CO_2 equivalents
COG	coke oven gas
FOB	free-on-board
GHG	greenhouse gas
GT	gas turbine
HHV	high heating value
HP	high pressure
IGCC	integrated gasification combined cycle
IP	intermediate pressure
LP	low pressure
MDEA	methyl diethanolamine
MEA	ethanolamine
NG	natural gas
NPV	net present value
ST	steam turbine

Roman and Greek symbols

A	heat exchange area (m^2)
AF	annuity factor
a, b	factors of calculating enthalpy
C	cost ($)
CCA	cost of CO_2 avoided ($/t$CO_2$e.)
γ	split fraction
F_L	tube length correction of heat exchangers
$F_{m,HX}$	heat exchanger material factor
$F_{m,pump}$	pump material factor
$F_{p,HX}$	heat exchanger pressure factor
$F_{t,motor}$	electric motor type factor
$F_{t,pump}$	pump type factor
m	mass flow rate (kg/hr)
N	number of compressor stages
η	efficiency of the equipment
ΔT_{LM}	log mean temperature difference
H	pump head (ft)
$Hp_{pump,j}$	horse power consumption of pump (hp)
h	enthalpy of stream (J/kg)
p	pressure (bar)
P	shell side pressure (psig)
PPP	purchasing power parity
Q	duties of utility (GJ/hr)
r	reducetion rate
R_{CO_2}	revenue from carbon tax ($)
S	shape factor
t	life time (year)
T	stream temperature (°C)
Tax_{CO_2}	carbon tax ($/ t CO_2e)
TCI	total capital investment ($)
TFC	total fixed cost ($)
TOC	annua operation cost ($)
TPC	total production cost ($)
TR	total revenue ($)
U	heat transfter coefficient (cal/sec-cm^2-k)
V	water flow rate (gallon/min)
W	work (kw)
ω_{CO_2}	carbon intensity in ecletric grid (tonne/kwh)
x_{cw}	price of cooling water ($/GJ)
$x_{elec.}$	Price of condenser utilities ($/GJ)
x_{cond}	electricity price ($/kwh)
x_{MDEA}	MDEA solvent price ($/kg)
x_{reb}	Price of reboiler utilities ($/GJ)
y	payback period (yr)

Subscripts and superscripts

add.	additional
air	air
B	base cost
ccpp	combined cycle power plant

$comb$	combustor
$comp$	compressor
cond	condenser
cool	cooling process
$current$	current sinario
$elec.$	electricity
g	exhaust gas
GT	gas turbine
H_2O	water or steam
HX	heat exchanger
i	number of heat exchanger
in	inlet
j	number of pump
k	LP, IP, and HP steam turbine
l	set of streams whose enthalpy are linear modeled
MDEA	MDEA solvent
motor	electric motor
new	updated cost index
old	original cost index
out	outlet
$pump$	pump
reb.	Reboiler
SQ	status quo
ST	steam turbine

References:

[1] Tony Valeri. Facility and GHG information,

http://ec.gc.ca/ges-ghg/donnees-data/index.cfm?do=facility_info&lang=En&ghg_id=G10091&year=2012#; 2017 [accessed Aug. 2017].

[2] Results of GHG Facility Data Search, Ontario, 2015.

http://ec.gc.ca/ges-ghg/donnees-data/index.cfm?do=results&lang=en&year=2015&gas=all&fac_name=&prov=ON&city=&naics=all&submit=Submit&order_field=data_co2eq&order=DESC.

[3] Technical Paper on the Federal Carbon Pricing Backstop,

https://www.canada.ca/en/services/environment/weather/climatechange/technical-paper-federal-carbon-pricing-backstop.html. ISBN 978-0-660-08506-7. [accessed 9 June 2017].

[4] Hamid Ghanbari; Frank Pettersson; Henrik Saxén. Sustainable Development of Primary Steelmaking under Novel Blast Furnace Operation and Injection of Different Reducing Agents. Chem. Eng. Sci. 2015, 129, 208–222.

[5] Hamid Ghanbari; Henrik Saxén; Ignacio E. Grossmann. Optimal Design and Operation of a Steel Plant Integrated with a Polygeneration System. J. AIChE. 2013, 59.10, 3659–3670.

[6] José M. Bermúdez; Ana Arenillas; Rafael Luque; J Angel Menéndez. An overview of novel technologies to valorise coke oven gas surplus. Fuel Process. Technol. 2013, 110, 150-159.

[7] Emissions, C. O. Tracking Industrial Energy Efficiency and CO2 Emissions. IEA,

https://www.researchgate.net/profile/Kanako_Tanaka2/publication/279804486_IEA_Tracking_Industrial_Energy_Efficiency_and_CO2_Emissions/links/576c7de608ae193ef3a9a56a.pdf; 2007 [accessed 20 Oct. 2017].

[8] Worldsteel association. World steel in figures 2017,

https://www.worldsteel.org/; 2017 [accessed 17 July 2017].

[9] Weizhu Shi; Liansuo An; Haiping Chen; Xuelei Zhang. Performance Simulation of Gas Turbine Combined Cycle with Coke Oven Gas as Fuel. APPEEC, 2009, DOI: 10.1109/APPEEC.2009.4918594

[10] Wei-Hua Yang; Tao Xu; Wei Li; Guang Chen; Li-yue Jia; Yue-jiao Guo. Waste gases utilization and power generation in iron and steel works. IITAW. 2009, DOI: 10.1109/IITAW.2009.107.

[11] Nai-Jun Zhou; Ai-Min Chen; Liang Luo; Yan-Li Li. Research and Application of Power Generation Schemes Using Coke Oven Gas. Energy Conservation Technology.2008, 26.3, 202-205.

[12] Guojie Zhang; Yue Dong; Meirong Feng; Yongfa Zhang; Wei Zhao; Hongcheng Cao. CO_2 reforming of CH_4 in coke oven gas to syngas over coal char catalyst. Chen. Eng. J. 2010, 156.3, 519-523.

[13] José M. Bermúdez; B. Fidalgo; A. Arenillas; J.A.Menéndez. Dry reforming of coke oven gases over activated carbon to produce syngas for methanol synthesis. Fuel. 2010, 89.10, 2897-2902.

[14] Yi Man; Siyu Yang; Yu Qian. Integrated process for synthetic natural gas production from coal and coke-oven gas with high energy efficiency and low emission. Energy Convers. Manag. 2016, 117, 162-170.

[15] Rauf Razzaq; Chunshan Li; Suojiang Zhang. Coke oven gas: availability, properties, purification, and utilization in China. Fuel. 2013, 113, 287-299.

[16] M. Modesto; S. A. Nebra. Exergoeconomic analysis of the power generation system using blast furnace and coke oven gas in a Brazilian steel mill. Appl. Therm. Eng. 2009, 29.11, 2127-2136.

[17] Zhibin Yang; Weizhong Ding; Yunyan Zhang; Xionggang Lu; Yuwen Zhang; Peijun Shen. Catalytic partial oxidation of coke oven gas to syngas in an oxygen permeation membrane reactor combined with NiO/MgO catalyst. Int. J. Hydrog. Energy. 2010, 35.12, 6239-6247.

[18] George T. Armstrong; Thomas L. Jobe.Jr. Heating values of natural gas and its components; Washington DC, 1982.

[19] Benxiong Yuan; Jinglong Liu. Desulphurization and Purification in CCPP Power Generation by Coke Gas. Shandong Chemical Industry. 2015, 44.17, 190-192.

[20] Michael A. Reynolds. Organometallic modeling of the hydrodesulfurization (HDS) process: rhenium carbonyl-promoted CS bond cleavage and hydrogenation of thiophenes and benzothiophenes. Dissertation, Iowa State University, 2002, 82-123.

[21] Zhu-rong Yang; Shou-hua Jian; Zhen-lin Wu; Yan-wei Yang. Discussion of feed gas purification technology for production of methanol from coke oven gas. Natural Gas Chemical Industry. 2011, 36.2, 42-45.

[22] O. Reg. 305/17. Environmental Protection Act: Ontario regulation 194/05, Industry emissions-nitrogen oxides and sulphur dioxide. R.S.O,

https://www.ontario.ca/laws/statute/90e19; 2017 [accessed 8 Sep. 2017]

[23] Thomas A. Adams II; Yaser K. Salkuyeh; Jake Nease. Reactor and Process Design in Sustainable Energy Technology, ed: Fan Shi. Chapter 6: Processes and Simulations for Solvent Based CO_2 Capture and Syngas Cleanup. 2014, 163–231.

[24] Hu Lin; Hongguang Jin; Lin Gao; Na Zhang. A polygeneration system for methanol and power production based on coke oven gas and coal gas with CO_2 recovery. Energy. 2014, 74, 174-180.

[25] Rolf Kehlhofer; Frank Hannemann; Bert Rukes; Franz Stirnimann. Combined-cycle gas & steam turbine power plants; Pennwell Books: Oklahoma, 2009.

[26] Renaud Gicquel. Energy systems: a new approach to engineering thermodynamics. Chapter 17: Combined Cycle Power Plants. CRC Press, 2011.

[27] Warren D. Seider; J.D. Seader; Daniel R. Lewin; Soemantri Widagdo. Product and Process Design Principles: Synthesis, Analysis and Evaluation; John Wiley & Sons, Inc., 2009.

[28] M. Boyce. Handbook for Cogeneration and Combined Cycle Power Plants; New York: American Society of Mechanical Engineers 1, 2004.

[29] M. Modesto; S. A. Nebra. Analysis of a Repowering Proposal to the Power Generation System of a Steel Mill Plant through the Exergetic Cost Method. Energy, 2006, 31.15, 3261–77.

[30] Mofid Gorji-Bandpy; Hamed Goodarzian. Exergoeconomic Optimization of Gas Turbine Power Plants Operating Parameters Using Genetic Algorithms: A Case Study. Thermal Science, 2011, 15.1, 43–54.

[31] The Chemical Engineering Plant Cost Index. Chemical Engineering,

http://www.chemengonline.com/pci-home; [accessed 5 June 2017].

[32] The wold bank data. PPP conversion factor, GDP (LCU per international $);

https://data.worldbank.org/indicator/PA.NUS.PPP?end=2016&name_desc=false&start=2016&view=bar; 2017 [accessed 10 Nov. 2017]

[33] Nye Thermodyamics Corp. Gas Turbine Prices by Output,

http://nyethermodynamics.com/trader/outprice.htm; 2017 [accessed 10 Nov. 2017].

[34] Allan R. Budris. The Impact of Component Material Selection on Pump Reliability, http://www.waterworld.com/articles/print/volume-30/issue-12/inside-every-issue/pump-tips-techniques/the-impact-of-component-material-selection-on-pump-reliability.html. [accessed 4 Oct. 2017]

[35] IESO. Price Overview,

http://www.ieso.ca/en/power-data/price-overview/global-adjustment; 2016 [accessed 10 Nov. 2017]

[36] IESO. Ontario Energy Report,

https://www.ontarioenergyreport.ca/pdfs/6001_IESO_Q4OER2016_Electricity_EN.pdf; 2013 [accessed 24 Nov. 2017].

[37] Peter Shawn Taylar. The Coming National Carbon Tax Gap. C2C Journal, http://www.c2cjournal.ca/2016/11/the-coming-national-carbon-tax-gap/; [accessed 23 May 2017].

[38] Eurostat statistics explained. Energy price statistics,

http://ec.europa.eu/eurostat/statistics-explained/index.php/Energy_price_statistics; 2017

[accessed 19 Oct. 2017].

[39] Hydro Quebec. Comparison of electricity prices in major North American cities,

http://www.hydroquebec.com/publications/en/docs/comparaison-electricity-prices/comp_2016_en.pdf; 2016 [accessed 20 Oct. 2017].

[40] The statistics portal. Global electricity prices by select countries in 2015 (in u.s. dollar cents per kWh, https://www.statista.com/statistics/263492/electricity-prices-in-selected-countries/; [accessed 14 Nov. 2017]

[41] Stephen Tindale. Carbon and Energy Taxes in Europe. Climate Answers.

http://climateanswers.info/2010/07/carbon-and-energy-taxes-in-europe/; [accessed 14 Nov. 2017]

[42] Worldbank. Population, Total,

http://data.worldbank.org/indicator/SP.POP.TOTL; [accessed 19 May 2017].

[43] Worldbank. CO_2 Emissions (Kt),

http://data.worldbank.org/indicator/EN.ATM.CO2E.KT; [accessed 19 May 2017].

[44] Worldbank. CO_2 Emissions from Electricity and Heat Production, Total (% of Total Fuel Combustion), http://data.worldbank.org/indicator/EN.CO2.ETOT.ZS; [accessed 19 May 2017].

[45] Worldbank. Electric Power Consumption (kWh per Capita),

http://data.worldbank.org/indicator/EG.USE.ELEC.KH.PC; [accessed 19 May 2017].

[46] Juan-Carlos Altamirano; Julia Martinez. Mexico's 3 Big Steps towards Comprehensive Carbon Pricing. World Resources Institute,

http://www.wri.org/blog/2017/04/mexicos-3-big-steps-towards-comprehensive-carbon-pricing;

[accessed 23 May 2017].

[47] U.S. Energy Information Administration. Electric power monthly,

https://www.eia.gov/electricity/monthly/epm_table_grapher.php?t=epmt_5_6_a; 2017 [accessed 20 Nov. 2017].

[48] Europe's Energy Portal. EU latest Energy Prices Report,

https://www.energy.eu/historical-prices/EU-Latest/; 2017 [accessed 20 Nov. 2017].

[49] Electricity Local. China Electricity Rates,

https://www.electricitylocal.com/states/texas/china/; 2016 [accessed 20 Nov. 2017].

[50] Worldsteel association, world steel in figures 2017,

https://www.worldsteel.org/en/dam/jcr:0474d208-9108-4927-ace8-4ac5445c5df8/World+Steel+in+Figures+2017.pdf; 2017 [accessed 23 Nov. 2017].

Appendix

Table A.1. Annual cost to operate the CCPP

Annual operation (hr)	*8000*		
Operations (labor-related)			*463800*
Direct wages and benefits (DW&B)	35	$/hr	*280000*
Direct salaries and benefits	15	% of DW&B	*42000*
Operating supplies and services	6	% of DW&B	*16800*
Technical assistance to manufacturing			*60000*
Control laboratory			*65000*
Maintenance (M)			
Wages and benefits (MW&B)	13	% of C_{TDC}	
Fluid handling process	3.5	% of C_{TDC}	
Solids-fluids handling process	4.5	% of C_{TDC}	
Solids-handling process	5	% of C_{TDC}	
Salaries and benefits	25	% of MW&B	
Materials and services	100	% of MW&B	
Maintenance overhead	5	% of MW&B	
Operating overhead			
General plant overhead	7.1	% of M&O-SW&B	
Mechanical department services	2.4	% of M&O-SW&B	
Employee relations department	5.9	% of M&O-SW&B	
Business services	7.4	% of M&O-SW&B	
Property taxes and insurance	2	% of C_{TDC}	
Depreciation			
Direct plant	8	% of (C_{TDC}-1.18 C_{alloc}	
Allocated plant	6	% of 1.18 C_{alloc}	
Rental fees			
Licensing fees			

Cost of Manufacture (COM)	the sum of the above from DW&B	
General Expenses		
Selling (or transfer) expense	3	% of sales
Direct research	4.8	% of sales
Allocated research	0.5	% of sales
Administrative expense	2	% of sales
Management incentive compensation	1.25	% of sales
Total general expenses (GE)		
Total Production cost (C)	TPC = COM+GE	

*Note: C_{alloc} is the allocated costs for utility plants and related facilities; % of sales is the % of total revenue (TR).

Table A.2. Factors for total capital investment

F.O.B. (Purchase) Costs	C_{fob}	Historical charts
Installation Costs	C_{inst}	$0.714*C_{fob}$
Construction Costs (Incl. Labor)	C_{cons}	$0.63*C_{fob}$
Total Direct Costs	C_{TDC}	$C_{TDC}=C_{fob} + C_{inst} + C_{const}$
Shipping (Incl. Insurance & Tax)	C_{ship}	$0.08*C_{fob}$
Construction Overhead	C_{over}	$0.571*C_{fob}$
Contractor Engineering	C_{engn}	$0.296*C_{fob}$
Contingencies	C_{slop}	$0.15 - 0.35*C_{fob}$
Total Indirect Costs	C_{TIC}	$C_{TIC}=C_{ship} +C_{over}+C_{engn}+C_{slop}$
Total Depreciable Capital	C_{dep}	$C_{dep}=C_{TDC}+C_{TIC}$
Land (Pure Real Estate)	C_{land}	$0.02*C_{dep}$
Royalties	C_{royle}	$0.02*C_{dep}$
Startup Costs	C_{strt}	$0.02\text{-}0.3*C_{dep}$ (often 0.1)
Fixed Capital Investment	C_{FCI}	$C_{FCI}=C_{dep}+C_{land}+C_{royl}+C_{strt}$
Cash Reserves	C_{cash}	8.33% of total annual expense
Inventory	C_{inv}	1.92% of annual tangible sales
Accounts Receivable	C_{recy}	8.33% of total annual revenue
Accounts Payable	C_{payb}	8.33% of annual tangible expenses

Total Working Capital	C_{wc}	sum of this section 0.7-0.89*(C_{fob}+C_{ship})
Total Capital Investment	C_{TCI}	(total FCI and working capital) $C_{TCI} = C_{FCI}+C_{WC}$

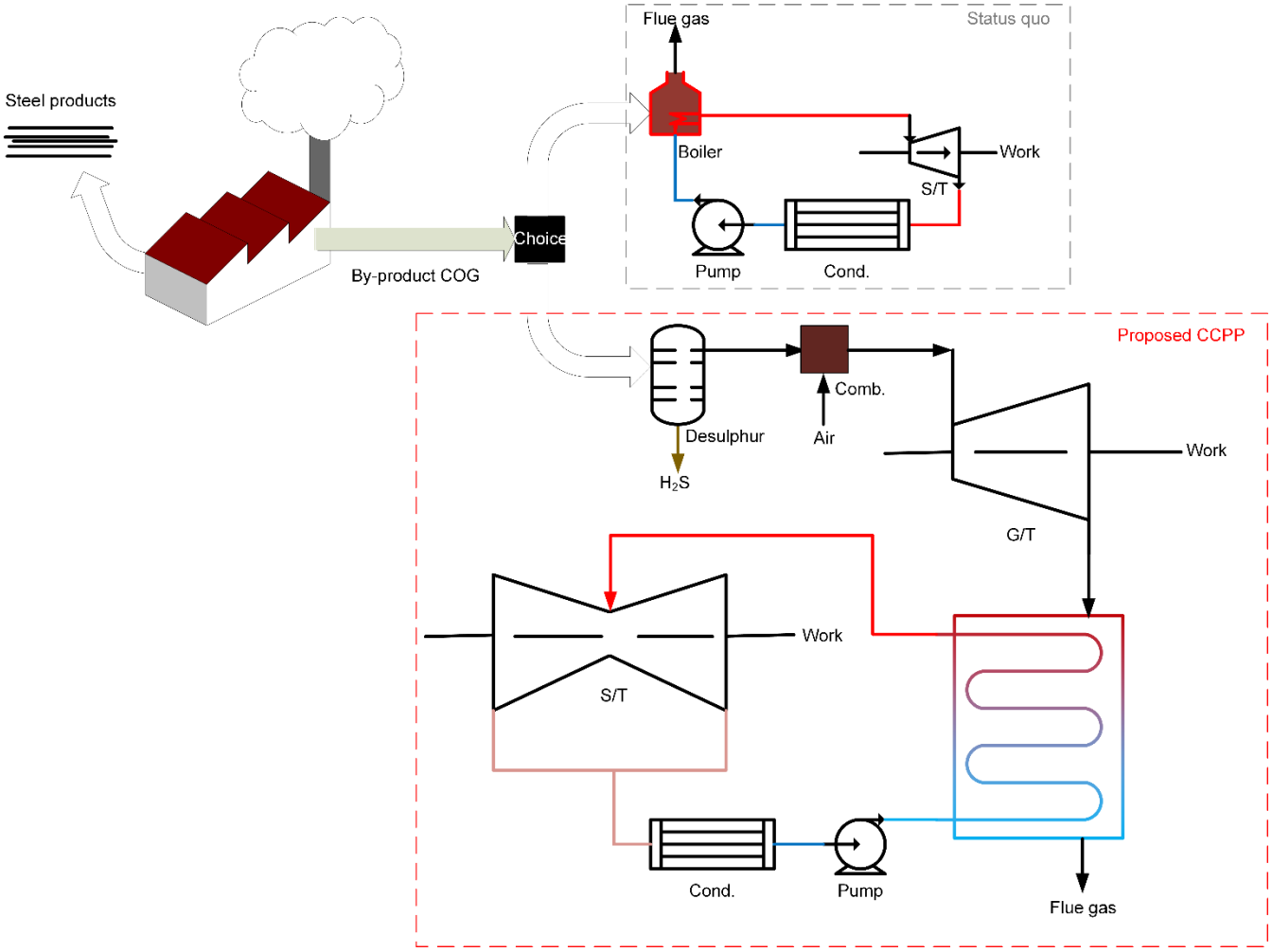
Steel products
By-product COG
Choice
Flue gas
Status quo
Boiler
Work
S/T
Pump
Cond.
Proposed CCPP
Desulphur
H_2S
Comb.
Air
Work
G/T
Work
S/T
Cond.
Pump
Flue gas

TOC